International Journal of GEOMATE, Oct., 2016, Vol. 11, Issue 26, pp.2534-2540
Geotec., Const. Mat. & Env., ISSN: 2186-2982(Print), 2186-2990(Online), Japan

EXPERIMENTAL STUDY ON THE EPS-BASED SHOCK ABSORBER FOR ROCK-SHED

Shen-Hsiang Hsu[1], Koji Maegawa[2] and Li-Hsien Chen[3]

[1,2]Graduate School of Natural Science and Technology, Kanazawa University, Japan
[3]Department of Civil Engineering, National Taipei University of Technology, Taiwan

ABSTRACT: Shock absorber made of piled up expanded polystyrene (EPS) placing above the roof of rock-shed is commonly use to advance the impact capacity against rockfall, but the require thickness increases with the accompanying rockfall energy and results in high construction cost or leads to the decrease of building amount. A new type of EPS-based shock absorber that composed of two EPS-blocks, surrounded by cage wire netting, then a steel grid placed onto was tested under a series of static and impact load tests in this study to find out its properties. Test results of static load tests show that strength increased about 20 % at the later stage, and force diffused more uniform due to the stiffness of steel grid. The results of impact load tests indicate that the limit capacity of impact energy in the EPS-based shock absorber is around 502.3 - 627.2 kJ, which is 50 % less than the empirical formula suggested by a rockfall mitigation code.

Keywords: Rockfall, Rock-shed, Shock absorber, EPS, Steel grid

1. INTRODUCTION

Rockfall is one of the natural disasters that result in severe consequents of the same level as loss of life induced by other slope disasters, it often occurs and strikes to transportation routes, railways, or underlying infrastructures in mountainous terrain. To protect lives and properties from those threats, various rockfall prevention and protection methods have been developed then constructed in numerous fields in recent years, but a rock-shed, however, is still referred to as the most secure, reliable method due to its shelter-shaped structure as well as having the highest rockfall energy capacity among all [1].

Rock-shed, a structure that is usually made up of reinforced concrete or shaped steel, then covered by shock absorber such as sand cushion, is usually installed at steep slope area where space alongside the road is insufficient to protect from direct rockfall and is especially efficient against a rockfall with high falling energy. However, as the volume or the falling height of a rock increased, enlarging the cross section of main structure as well as thickening the shock absorber above a rock-shed are some general ways to withstand higher rockfall impact, but the bulk volume also incurs high construction cost in the same time. On this condition, expanded polystyrene (EPS) has been employed as a type of shock absorber due to its light weight, easily deform, long-term durable and incombustible characteristics. Although having the great advantage of shock absorbing function, EPS material is still limited in load distribution effect and is easy to scatter while being impacted by rockfall. Thus, a shock absorber which is able to improve those mentioned disadvantages and could reduce the cross section of rock-shed to lower the total construction cost, is expected to be developed.

To distribute and absorb impact load of rockfall, then consequently transmit a less impact load to the main structure of rock-shed, a new type of shock absorber dominated by EPS material with a combination of steel grid, which named the EPS-based shock absorber, is introduced in this study. The design of the EPS-based shock absorber is eager to promote distribution effect by the stiffness of the steel grid, and to simplify design work by confirming the energy capacity against a falling rock. Therefore, a series of static load tests which carried out by using a testing machine, and full-scale impact load tests by dropping blocks of different weights onto test specimens as well have conducted to find out the properties of the EPS-based shock absorber in this study.

2. COMPOSITION OF THE EPS-BASED SHOCK ABSORBER

The EPS-based shock absorber is composed of steel grid and framed EPS, of which the framed EPS is composed of two EPS-blocks, surrounded by cage wire netting, piling up from 1 to 3 layers in a crisscross way, as shown in Fig. 1. The adoption of steel grid here is used to widen the distributed range of impact load due to its great stiffness, whereas the cage wire netting is expected to connect several framed EPS together, and to offer better coverage to prevent EPS-blocks from scattering while being impacted. Moreover, a 0.5 m thick sand cushion will cover it at practical application.

Configurations of the main components in the EPS-based shock absorber are listed below. The steel grid is composed of several steel sheets and steel bars of SS400, and the size is 2.05 m long, 2.05 m wide, and 0.1 m high. The EPS-block of which unit weight is 16 kg/m^3 is applied, and the size of a block is 2.0 m long, 1.0 m wide, and 0.5 m thick, so a framed EPS approximately becomes the size of length 2.05 m, width 2.05 m, and thickness 0.52 m. The cage wire netting is made of 300 g/m^2 aluminum-zinc coating steel wires to withstand the natural corrosion, and with the size of 4.0φ-75×75.

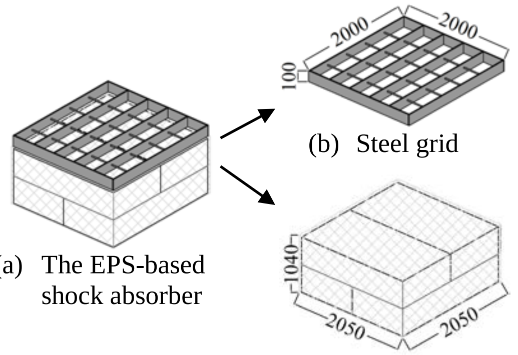

(a) The EPS-based shock absorber

(b) Steel grid

(c) Framed EPS

Fig. 1 Composition of the shock absorber

3. OUTLINE OF THE TESTS ON THE EPS-BASED SHOCK ABSORBER

3.1 Static Load Tests

Static load tests were carried out on eight EPS-based shock absorber specimens by using a testing machine loading at the center position of a test specimen, as shown in Fig. 2. A loading plate of 1.0 m in diameter was conservatively adopted due to a rock weighed 1.0 ton has an equivalent diameter of about 0.9 m. The static load was applied through the loading plate and was gradually increased until specimen approached a goal of 80 - 90 % strain, which had been regarded as the limit state in accordance with the former research [2].

Table 1 shows the eight specimens composed of different materials. The specimens are categorized into three test series: Composition of test specimens in test series SE1 are framed EPS, but are different in piling layers. A steel grid is placed onto the same framed EPS structure of different layer amount in test series SE2. And in test series SE3, an extra framed EPS is set in each layer, hence requires a two times longer steel grid with the size of 4.0 m long, 2.0 m wide, and 0.1 m thick.

Load and displacement amounts were measured by the load cell and the stretch of stroke built inside the testing machine with hydraulic servomechanism, for the purpose of obtaining the stress-strain relationships of test specimens.

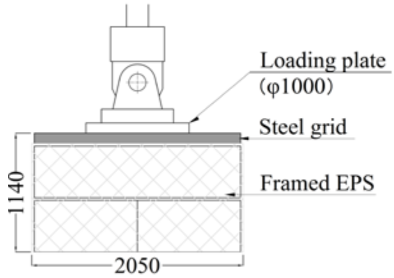

Fig. 2 Schematic view of static load test

Table 1 Specimen compositions of static load tests

Case No.	Composition of specimen	Layer of framed EPS	Remark
SE1-1	Framed EPS	1	1 framed EPS in each layer
SE1-2		2	
SE1-3		3	
SE2-1	Framed EPS & Steel grid	1	1 framed EPS in each layer
SE2-2		2	
SE2-3		3	
SE3-1	Framed EPS & Steel grid	1	2 framed EPSs in each layer
SE3-2		2	

3.2 Impact Load Tests

Impact load tests were carried out by dropping a block vertically onto the center position of a test specimen, as shown in Fig. 3. The block of which shape was specified in the guideline ETAG 027 [3] was used in the tests and was made of reinforced concrete wrapped with steel plates.

Three full-scale impact load tests with impact energies of 502.3, 642.9, and 1029.0 kJ, which are respectively generated from block masses and falling heights of 2.5 ton - 20.5 m, 3.2 ton - 20.5 m, and 4.2 ton - 25.0 m in cases no. DE1, DE2, and DE3, are listed in Table 2. Besides, the same specimen utilized in the tests has a configuration as shown in Fig. 3. It is composed of eighteen framed EPSs assembled in a 3 by 3 way and piled up crisscross with two layers. Then, six pieces of bolt-connected steel grids with each size of 2 m × 3 m are placed on the framed EPSs, and finally, a sand cushion of 0.5 m thick is set on the top of those steel grids to cut off the ultraviolet from sunlight which might do harm to the EPS material.

The main measuring item and measuring method in the impact load tests are listed below:

1. Block acceleration: a transceiver, a tri-axial accelerometer, and an amplifier-recording device were set into the center of the block to receive a trigger signal and record the acceleration data at a sampling rate of 2 kHz [4].
2. Transmitted impact load to floor concrete: 13 earth pressure cells (#1~#13) were set on the base concrete at 900 mm interval, and the plan view is as shown in Fig. 4.

3. Test condition: several normal and high-speed video cameras were set up in the front and the lateral sides of the test specimen.

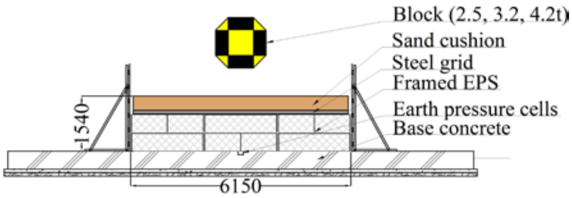

Fig. 3 Schematic view of impact load tests

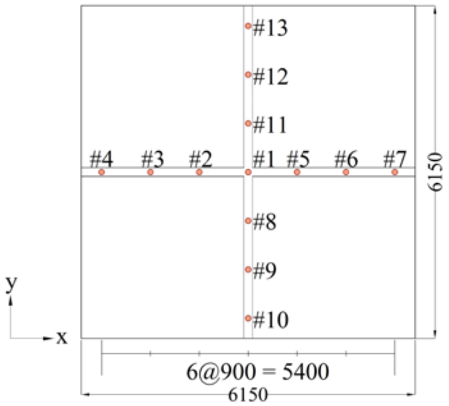

Fig. 4 Plan view of earth pressure cells' locations

Table 2 Impact energies used in impact load tests

Case No.	Block mass (ton)	Falling height (m)	Impact energy (kJ)
DE1	2.5	20.5	502.3
DE2	3.2	20.5	642.9
DE3	4.2	25.0	1029.0

4. RESULTS OF THE EPS-BASED SHOCK ABSORBER TESTS

4.1 Results of Static Load Tests

In order to compare with the stress-strain relationship of EPS material mentioned in the former research [2], a pure EPS-block with the size of 80 mm long, 80 mm wide, and 160 mm high was measured under a compression test then plotted as a dotted line shown in Figs. 5 and 6.

Figure 5 shows the stress-strain relationships of framed EPS and pure EPS. Comparing the curves of case no. SE1-1 and pure EPS, tendencies of both are similar but framed EPS has relatively weak stiffness at the early stage of loading. It was likely to cause by the gap between cage wire netting and EPS-block. Therefore, after cage wire netting was embedded into EPS-block in the test process, the stress of framed EPS slightly expanded in the elastic domain, and eventually became about 20 % higher than that of pure EPS at 70 % strain. Although a cage wire netting might cause a difference of stresses between framed EPS and pure EPS-block, the difference is much possible to cause by the force diffused inside framed EPS due to its dimensions being considerably larger than that of a loading plate [5]. The reason is evident as follows.

After tests, in cases no. SE1-1 to SE1-3, an L_1 = 1100 mm diameter punching shear failure area were found on the top surface of the 1st framed EPS layer in all cases, as shown in Fig. 7. On the surface of the 2nd layers in cases no. SE1-2 and SE1-3, L_2 = 1600-1700 mm diameter deformation area were observed. And on the 3rd surface layer of framed EPS in case no. SE1-3, L_3 = 2000 mm diameter ─ an entire smooth deformation on framed EPS ─ was observed. According to these results, the area changing between the layers were restricted by the boundary of the specimen, but approximately a 30-degree stress distribute angle which was the same as in the EPS material [2] could still be found in the framed EPS.

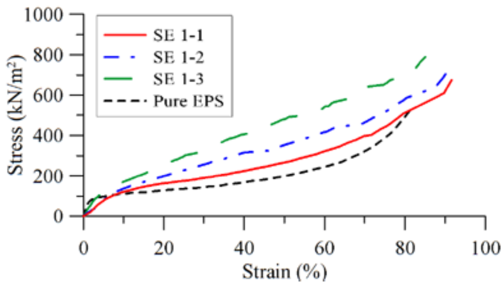

Fig. 5 Stress-strain curves of framed EPS and pure EPS

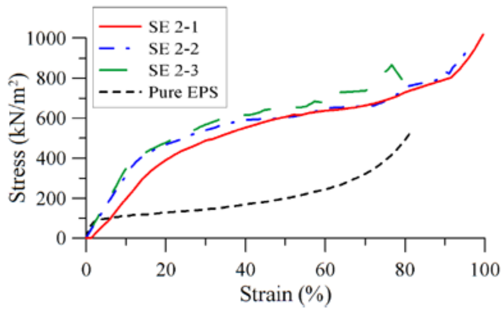

Fig. 6 Stress-strain curves of the EPS-based shock absorber and pure EPS

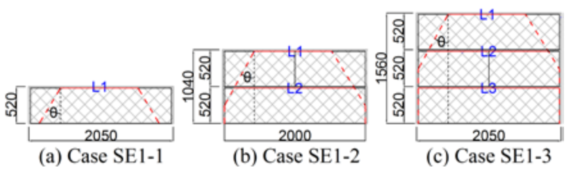

Fig. 7 Stress distribution inside framed EPS

Figure 6 shows the stress-strain relationships of the EPS-based shock absorber and pure EPS. In cases no. SE2-1 to SE2-3, stresses in elastic domain increased about 4-5 times due to the high stiffness of the steel grid, and strains in elastic domain gained to 10 - 20 %. But because of the utilization of steel grid, force spread sufficiently on the framed EPS, the influence of its piling amount was not obvious, even test series SE3 showed the same result. These facts are also clear from visual recognition: Fig. 8(b) shows a continuous and uniform deformation appears in the entire EPS-based shock absorber, which substitutes for a punching shear failure on the surface of framed EPS in Fig. 8(a). But in case no. SE3-2, both longitudinal ends are tilted and make discontinuous deformation, as shown in Fig. 8(c). The deformation area on the surface of framed EPS in case SE3-2 was about 2000 mm diameter, which indicate that steel grid extended about 1000 mm wider than the loading plate.

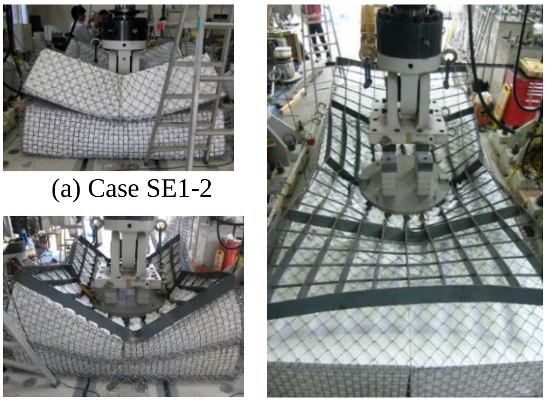

(b) Case SE2-2 (c) Case SE3-2

Fig. 8 Deformation condition of test specimens

4.2 Results of Impact Load Tests

According to the measurements in impact load tests, test condition could reappear through the images captured by high-speed cameras. Besides, by the data obtained from accelerometer and earth pressure cells, two quantities are respectively defined as follow. (1) Impact load: acquired from multiplying block mass by block acceleration. (2) Transmitted impact load: acquired from the integration of earth pressure. Results of impact load tests are shown in the following sections.

4.2.1 Behavior of the EPS-based shock absorber

Take case no. DE2 for example, Fig. 9 shows the process of impacting captured by the high-speed camera. After a block been released by a rafter crane, the time it contacted with the surface of the sand cushion was set as 0 ms. The block then penetrated to the maximum depth after 90 ms, and then rebounded to the maximum height at 717 ms. Finally, a still image was taken at 3000 ms.

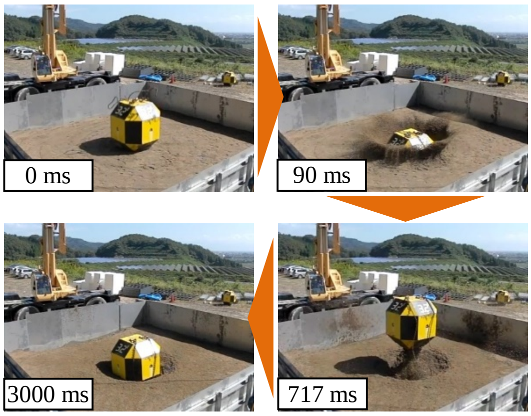

Fig. 9 Process of block impact

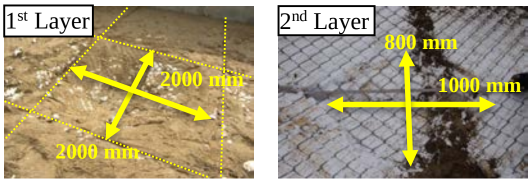

Fig. 10 Deformation of framed EPS in case DE3

In addition, consider the deformation range of each layer of the EPS-based shock absorber. Deformation area in steel grid was larger than in sand cushion, but was then shrunk to the centerpieces of framed EPS in all cases. This phenomenon indicates that, though the utilization of steel grid was eager to distribute much load to the material below, the distributed effect was still limited by the gap between two framed EPS. Moreover, a local shear failure area of was found on the second surface of framed EPS in case DE3.

4.2.2 Impact load and transmitted impact load

Figures 11~13 show a combination of load and time curves in cases DE1 to DE3, of which the solid curves represent impact load, and the dotted curves represent transmitted impact load. Additionally, a value of impact load acting through a 90 cm thick sand cushion is calculated by the empirical formula Eq. (1), and is added for comparison [6].

$$P_{max} = 2.108 \cdot (m \cdot g)^{\frac{2}{3}} \cdot \lambda^{\frac{2}{5}} \cdot H^{\frac{3}{5}} \cdot \alpha \qquad (1)$$

where P_{max}, m, g, λ, H, T and D represent impact load (kN), mass of a block or a falling rock (t), gravitational acceleration (m/s^2), Lame's constant (kN/m^2), falling height (m), thickness of sand cushion (m), and diameter of a block (m), respectively. Lame's constant equals to 1000 kN/m^2 while using a soft material such as sand cushion. Besides, the overdesign factor α which equals to $(T/D)^{-0.5}$ should be considered when the equivalent diameter of a block is greater than the thickness of sand cushion [1].

In Figs. 11~13, about two waves could find in each impact load curve. The first wave begins at a block contact with the surface of the sand cushion, and the second wave stands for cushioning action. Figs. 11 and 12 both show that the maximum value of transmitted impact load appears about 25 ms later than impact load. But in Fig. 13, both values happen almost at the same time. It is supposed to affect by the local shear failure on the second surface of framed EPS, which indicates that 1029.9 kJ rockfall energy has probably exceeded the limit capacity of the EPS-based shock absorber.

Comparing with the transmitted impact load at 90 cm thick sand cushion, Table 3 indicates that the EPS-based shock absorber could reduce about 65 or 50 % impact load while facing a 502.3 or a 642.9 kJ rockfall energy respectively. As a result, falling energy around 502.3 - 642.9 kJ is supposed to be the limit capacity that the EPS-based shock absorber could still remain its cushioning function.

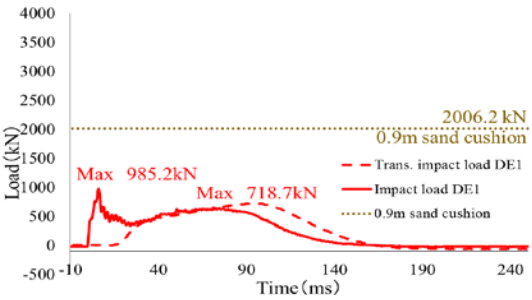

Fig. 11 Load-time curves in case DE1 (502.3 kJ)

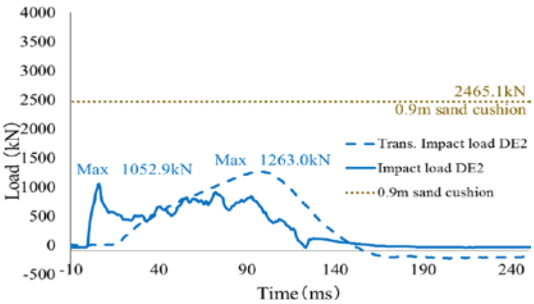

Fig. 12 Load-time curves in case DE2 (642.9 k)

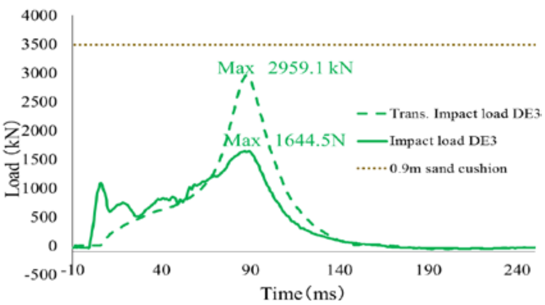

Fig. 13 Load-time curves in case DE3 (1029.0 kJ)

Table 3 Results of impact load test

Case No.	Maximum impact load (kN)	Maximum transmitted impact load (kN)	Impact load at 90 cm sand cushion (kN)
DE1	985.2	718.7	2006.2
DE2	1052.9	1263.0	2465.1
DE3	1644.5	2959.1	3482.7

Figures 14, 16, and 18 show a combination of stress- and depth-duration curve of the first impact measured by earth pressure cells and accelerometer. Results of 13 earth pressure cells are all plotted in the figures, where thick lines represent the center (#1) and others adjacent to it (#2, #5, #8, and #11) because of having better earth receiving results, but the others are plotted in thin gray lines. By the result, it shows that earth pressures are detected in an 1800 mm diameter range where the areas are similar to a piece of framed EPS. Meanwhile, the depth-duration curves reveal the penetration behaviors while being impact, but the curve in case DE2 shows a bad convergence behavior which must have come from the inclination of the accelerometer [7]. In addition, though the maximum earth pressure was supposed to be detected by the center earth pressure cell (#1), results such as Fig. 14 and Fig. 16 are likely to be influenced by the composition of a framed EPS because the center earth pressure cell was exactly located beneath the interface of two EPS-blocks inside. But in Fig. 18, the local shear failure on the second surface of framed EPS seems to result in an obvious stress concentration behavior.

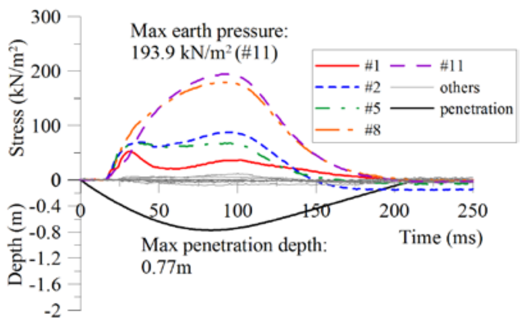

Fig. 14 Stress, depth duration curves in case DE1

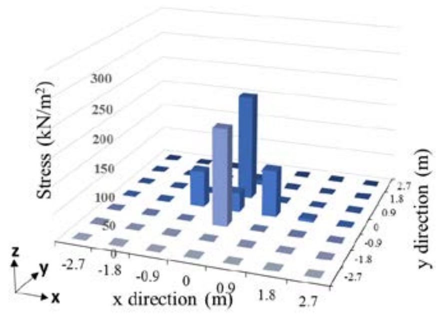

Fig. 15 Stress distribution in case DE1 (at 95 ms)

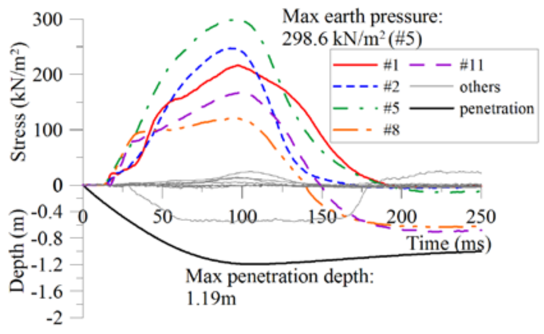

Fig. 16 Stress, depth duration curves in case DE2

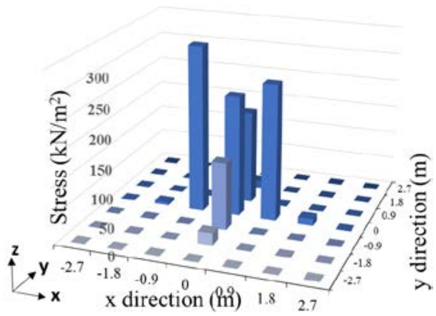

Fig. 17 Stress distribution in case DE2 (at 98 ms)

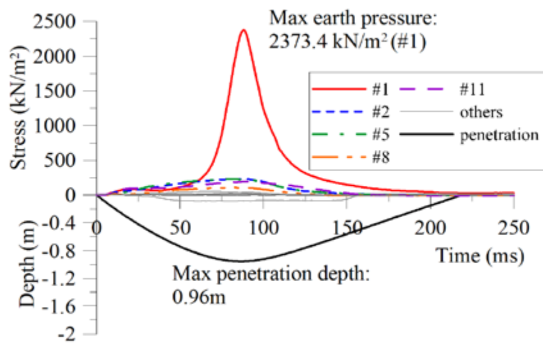

Fig. 18 Stress, depth duration curves in case DE3

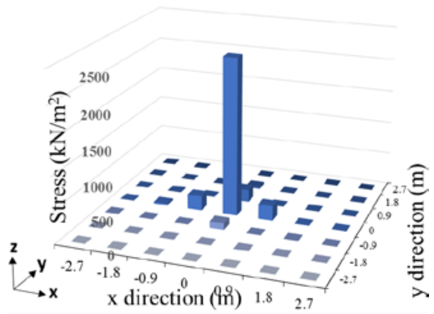

Fig. 19 Stress distribution in case DE3 (at 88 ms)

Figs. 15, 17, and 19 show the stress distribution conditions at the moment of maximum integrated earth pressure amount. The plane axis represents the distribution points of earth pressure cells, and the z-axis stands for detected stress. Figs. 15 and 17 once again show clear evidence that stress is well distributed around the impact positions, but the center point does have relatively low earth pressure. But in Fig. 19, stress concentrates on the center point and is about 10 times greater than the others.

CONCLUSION

The main results of static and impact load tests on the EPS-based shock absorber are listed below.

1. Framed EPS, composing of two EPS-blocks surrounded by cage wire netting, seems to have about 20% greater performance in strength than pure EPS at the late stage of static load test in this study. However, the result is more likely to cause by the force diffused inside a framed EPS due to its dimensions is much larger than a loading plate.
2. Results of static load tests show that, the force spreads sufficiently on framed EPS owing to the utilization of a steel grid, so the stress increases about 4-5 times in elastic domain of the EPS-based shock absorber.
3. The limit capacity of falling energy in the EPS-based shock absorber is around 502.3 - 627.2kJ.
4. While facing rockfall energy lower than 642.9 kJ, the EPS-based shock absorber could reduce about 50 % impact load than a 90 cm thick sand cushion calculated by an empirical formula suggested by a rockfall mitigation code.
5. Due to the influence of the composition of framed EPS, stress concentrates at about a same area as framed EPS after impact.

ACKNOWLEDGEMENTS

Special thanks to Raiteku Corporation Limited and all the relevant partners for the cooperation and all kinds of support during these tests.

REFERENCES

[1] Japan Road Association, “Rockfall Mitigation Handbook (in Japanese)”, Maruzen, 2000.
[2] Yoshida H., Fujii T., Minami K. and Maegawa K., “Experimental Study on Shock Absorbing Characteristic of Reinforced Expanded Polystyrol against Falling Rocks (in Japanese)”, Proceedings of the Symposium on Impact Problems in Civil Engineering, Vol. 4, pp.6-11, 1998.
[3] ETAG 027, “Guideline for European Technical Approval of Falling Rock Protection Kits”, European Organisation for Technical Approvals (EOTA), 2000.
[4] Tran PV and Maegawa K., “Experiments and Numerical Modeling of a Rockfall Protective Wire Rope Fence”, International Journal of GEOMATE, Vol.2, Sl.4, pp.2186-2990, 2012.

[5] Alkroosh I. and Nikraz H., "Evaluation of Pile Lateral Capacity in Clay Applying Evolutionary Approach", International Journal of GEOMATE, Vol.4, Sl.7, pp.462-465, 2013.
[6] Kishi N., Nakano O., Matsuoka K. and Nishi H., "Field Test on Absorbing Capacity of Sand Cushion (in Japanese)", Journal of Structural Engineering, Vol. 39 A, pp.1587-1597, 1993.
[7] Adhilla Ainun Musir and Abdul Naser Abdul Ghani, "A Study of Pile Driving Effects on Nearby Building", International Journal of GEOMATE, Vol. 6, Sl.11, pp.806-810, 2014.

International Journal of GEOMATE, Oct., 2016, Vol. 11, Issue 26, pp.2534-2540.
MS No. 5130 received on June 16, 2015 and reviewed under GEOMATE publication policies.

Pertinent discussion including authors' closure, if any, will be published in Oct. 2017 if the discussion is received by April 2017.
Corresponding Author: Shen-Hsiang Hsu